NJC

PAPER

Synthesis of donor-substituted *meso*-phenyl and *meso*-ethynylphenyl BODIPYs with broad absorption†

Katja Gräf,[a] Thomas Körzdörfer,[b] Stephan Kümmel[b] and Mukundan Thelakkat*[a]

We report the synthesis of *meso*-ethynylphenyl BODIPYs and compare their properties with the corresponding *meso*-phenyl derivatives. Both types of BODIPYs carry a 2-cyano-3-acrylic acid anchoring moiety and either methyl groups or 4,4′-dimethoxytriphenylamine (MeOTPA) donor groups at positions 3 and 5. All compounds were characterized by NMR, UV/vis and cyclic voltammetry. The MeOTPA-substituted BODIPYs show an excellent panchromatic absorption with high molar extinction coefficients over the whole UV/vis range up to the near-IR region. The most impressive absorption was exhibited by the MeOTPA-substituted *meso*-ethynylphenyl BODIPY which strongly absorbs up to 1030 nm. By cyclic voltammetry measurements, all compounds were identified to be electrochemically stable in solution. Further, it was observed that the value of the LUMO level can be tuned by the *meso*-substituent. The HOMO level is determined by the donor substituents (-5.41 ± 0.03 eV and -4.84 ± 0.01 eV for BODIPYs with methyl groups and MeOTPA donor groups, respectively). These findings were further supported by DFT calculations. To evaluate the potential of the BODIPYs as sensitizers, the incident photon-to-current conversion efficiencies of solid-state dye-sensitized solar cells were measured. The photoaction spectra clearly show that the BODIPYs contribute to the photocurrent generation over their entire absorption region.

Introduction

The 4,4-difluoro-4-bora-3a,4a-diaza-*s*-indacenes, better known as BODIPYs,[1] have emerged as attractive compounds for many research areas, including the application as laser dyes,[2] biochemical labeling agents,[3] fluorescence sensors[4]/switches,[5] electroluminescent materials[6] or molecular photonics.[7] The large variety of applications of this class of dyes are based on their outstanding properties.[8–10] BODIPYs are thermally and photochemically stable, chemically robust, redox active and highly fluorescent. Most importantly, they are characterized by an intensive absorption profile in the visible region that can be easily tuned by chemical modification of the BODIPY core.[9] This feature makes these dyes highly interesting for the application as sensitizers in solar cells because it provides the opportunity to improve the light harvesting by the extension of the absorption. However, their use as sensitizers and donor

materials in solar cells is in its infancy and the efficiencies are still low. It has been shown that BODIPYs can be used as sensitizers in solid-state dye-sensitized solar cells,[11] liquid electrolyte dye-sensitized solar cells[12–14] and also as active material in organic bulk heterojunction solar cells.[15]

In the present work we focused on the structural modification of the BODIPY core to accomplish excellent optical properties with the goal of improving the light harvesting in solar cells. For this, panchromatic absorption behaviour accompanied by high extinction coefficients has to be realized. Therefore, we synthesized a series of BODIPY dyes differing in the *meso*-substituent and the groups at positions 3 and 5 (see **5**, **8**, **13** and **16**, Scheme 1). From the literature it is known that arylation at the *meso*-position affects the optical and electrochemical properties only marginally.[16] The reason for this is the orthogonal orientation of the *meso*-phenyl moiety relative to the planar BODIPY core. This configuration reduces the conjugation between the two units. To improve the conjugation and thus the extent of absorption, we introduced an ethynyl-bridge between the *meso*-phenyl group and the BODIPY core creating *meso*-ethynylphenyl BODIPYs (**13**, **16**). The idea was to enable an efficient delocalization due to the comparatively diffuse nature of the π-bonds of the ethynyl-bridge creating a cylindrical electron cloud around the σ-bond. Porphyrin chemistry has already shown

[a] University of Bayreuth, Macromolecular Chemistry I, Applied Functional Polymers, D-95447 Bayreuth, Germany. E-mail: Mukundan.Thelakkat@uni-bayreuth.de; Fax: +49 921 55 3109; Tel: +49 921 55 3108
[b] University of Bayreuth, Theoretical Physics IV, D-95447 Bayreuth, Germany
† Electronic supplementary information (ESI) available: Mechanisms of the Knoevenagel-type condensation, NMR-spectra, UV/vis-spectra, fluorescence-spectra, cyclic voltammetry data. See DOI: 10.1039/c3nj00157a

that ethynyl-type bridges can bring about strong electronic interactions between two connected moieties.[17] For the synthesis of such *meso*-ethynylphenyl BODIPYs, we successfully used the condensation of an alkynyl aldehyde with a pyrrole derivative. To further increase the extent of the absorption, we attached strong donor groups to the BODIPY core *via* vinylic bonds. To this end, 4,4′-dimethoxytriphenylamine (MeOTPA) was selected. MeOTPA is a strong donor due to the high electron density and the high lying HOMO level. It is also stable against oxidative coupling. Finally, a 2-cyano-3-acrylic acid anchoring moiety was attached to the each BODIPY dye making them suitable for the application in hybrid solar cells. The structural, optical, electrochemical and photovoltaic properties of the *meso*-phenyl (**5**, **8**) and *meso*-ethynylphenyl BODIPYs (**13**, **16**) bearing methyl or MeOTPA groups at positions 3 and 5 were compared. Their applicability as sensitizers for TiO_2 for light harvesting and energy conversion was tested in hybrid solar cells.

Results and discussion

Synthesis

The synthetic routes for the preparation of the target BODIPYs **5**, **8**, **13** and **16** are depicted in Scheme 1. The *meso*-phenyl derivatives **5** and **8** were prepared according to a conventional coupling method using an aromatic aldehyde (Scheme 1, route a).[14] Thus **5** and **8** were both obtained from **3**, which was synthesized from 4-(1,3-dioxolan-2-yl)benzaldehyde **1** and kryptopyrrole **2**. Deprotection of **3** and subsequent Knoevenagel condensation with 2-cyanoacetic acid resulted in the formation of **5**. For obtaining **8**, the MeOTPA-donor had to be attached first to **3**. Therefore, 4-(di(4-methoxyphenyl)amino)benzaldehyde was reacted with the methyl groups of **3** at the positions 3 and 5 by a Knoevenagel-type condensation to yield **6**. After the deprotection of the aldehyde functionality, the resulting compound **7** was condensed with 2-cyanoacetic acid to yield **8**.

For the synthesis of the *meso*-ethynylphenyl BODIPYs, we developed a novel route (Scheme 1, route b). These BODIPYs were synthesized starting from a non-aromatic aldehyde, *viz.* an alkynyl aldehyde (**9**). Typically aromatic aldehydes, acid chlorides or anhydrides are used for the preparation of BODIPYs. To the best of our knowledge, no alkenyl or alkynyl aldehydes have been used for this reaction. However, a comparable reaction route is already known from porphyrin chemistry where **9** was reacted with pyrrole to give the associated dipyrromethane and finally the *meso*-ethynyl porphyrin.[18,19] The *meso*-ethynylphenyl BODIPYs (**13** and **16**) were synthesized starting from kryptopyrrole **2** and the alkynyl aldehyde 3-(trimethylsilyl)-2-propynal **9** to give **10**. After deprotection of **10**, a Sonogashira coupling of **11** with the final 4-(2-carboxy-2-cyanovinyl)phenyl anchoring group **12** was performed to yield directly the *meso*-ethynyl-phenyl BODIPY **13**. To get the MeOTPA-substituted *meso*-ethynyl counterpart of **8**, the TMS-protected *meso*-ethynyl BODIPY **10** was used for the Knoevenagel-type condensation with 4-(di(4-methoxyphenyl)amino)benzaldehyde. To this end, the aromatic aldehyde was reacted with the 3,5-dimethyl BODIPY **10** in the presence of a piperidine/glacial acetic acid or a

piperidine/*p*-toluenesulfonic acid catalyst system in non-polar solvents such as benzene or toluene. The proposed mechanism of this reaction is presented in the ESI.† The basicity and nucleophilicity of the amine used generally determine the mechanism, either as the Hann–Lapworth (Fig. S1, ESI†) or the organocatalytic (Fig. S2, ESI†) mechanism; both being well-studied for a variety of such condensations.[20,21] For instance, the Hann–Lapworth mechanism is the only valid mechanism for reactions including tertiary amines because they cannot perform a nucleophilic attack on the carbonyl carbon of aldehydes as required in the organocatalytic mechanism. For reactions using primary or secondary amines either mechanism are conceivable and piperidine is a common secondary amine used for this reaction. But as we performed the reaction with 2,2,6,6-tetramethyl-piperidine (TMP) which is also a secondary amine and as basic as piperidine but much more bulky, we observed no reaction (even after one week under reflux). Similarly, by using the tertiary base NEt_3 (which has also a comparable basicity), we did not observe a condensation reaction. Thus bases with the comparable basicity as piperidine that are not able to activate the aldehyde did not promote the Knoevenagel condensation at all. Moreover, we isolated the aminal (structure B, Fig. S2 and S3, ESI†) expected in an organocatalytic route. From these results it can be deduced that the organocatalytic mechanism is relevant for the condensation between BODIPYs and donor aldehydes. The proposed mechanism in Fig. S2 (ESI†) is further supported by the exclusive formation of *trans*-substituted BODIPYs (see ^{1}H-NMR spectra of **8** and **16**, Fig. S4 and S5, ESI,† respectively). In this way, **14** could be synthesised from **10** in a Knoevenagel-type condensation. After deprotection of **14**, **15** was reacted with **12** in a Sonogashira coupling to afford **16**. All compounds were characterized using FT-IR, ^{1}H-NMR, UV/vis and cyclic voltammetry measurements.

Characterization by NMR

NMR analysis was used to investigate (1) the influence of the *meso*-substituent on the electronic and magnetic environment of the BODIPY scaffold, (2) the stereochemistry of the vinyl bonds and (3) the geometry of the 4-(2-carboxy-2-cyanovinyl)-phenyl anchoring unit.

The influence of the *meso*-substituent was examined by comparing the ^{1}H-NMR spectra of **18**, **3** and **17** (Fig. 1, full spectra in Fig. S7, ESI†) differing only in the substituent at the *meso* position: *meso*-proton, *meso*-phenyl and *meso*-ethynylphenyl. The main difference between *meso*-phenyl and *meso*-ethynyl-phenyl BODIPYs is the chemical shift of the resonance signal assigned to the 1,7-methyl groups of the BODIPY core. These occur at about 1.28 ppm for *meso*-phenyl derivatives (*e.g.* **3**), whereas they occur at about 2.53 ppm for the *meso*-ethynyl-phenyl BODIPYs (*e.g.* **17**). This gives clear evidence that the chemical and/or magnetic environment of these protons is strongly influenced by the substituent at the *meso*-position. Relative to the corresponding *meso*-proton compound **18**, the orthogonal phenyl moiety in **3** seems to increase the electron density and hence the shielding of the 1,7-methyl groups. The interesting resonance signal appears at a distinctly lower
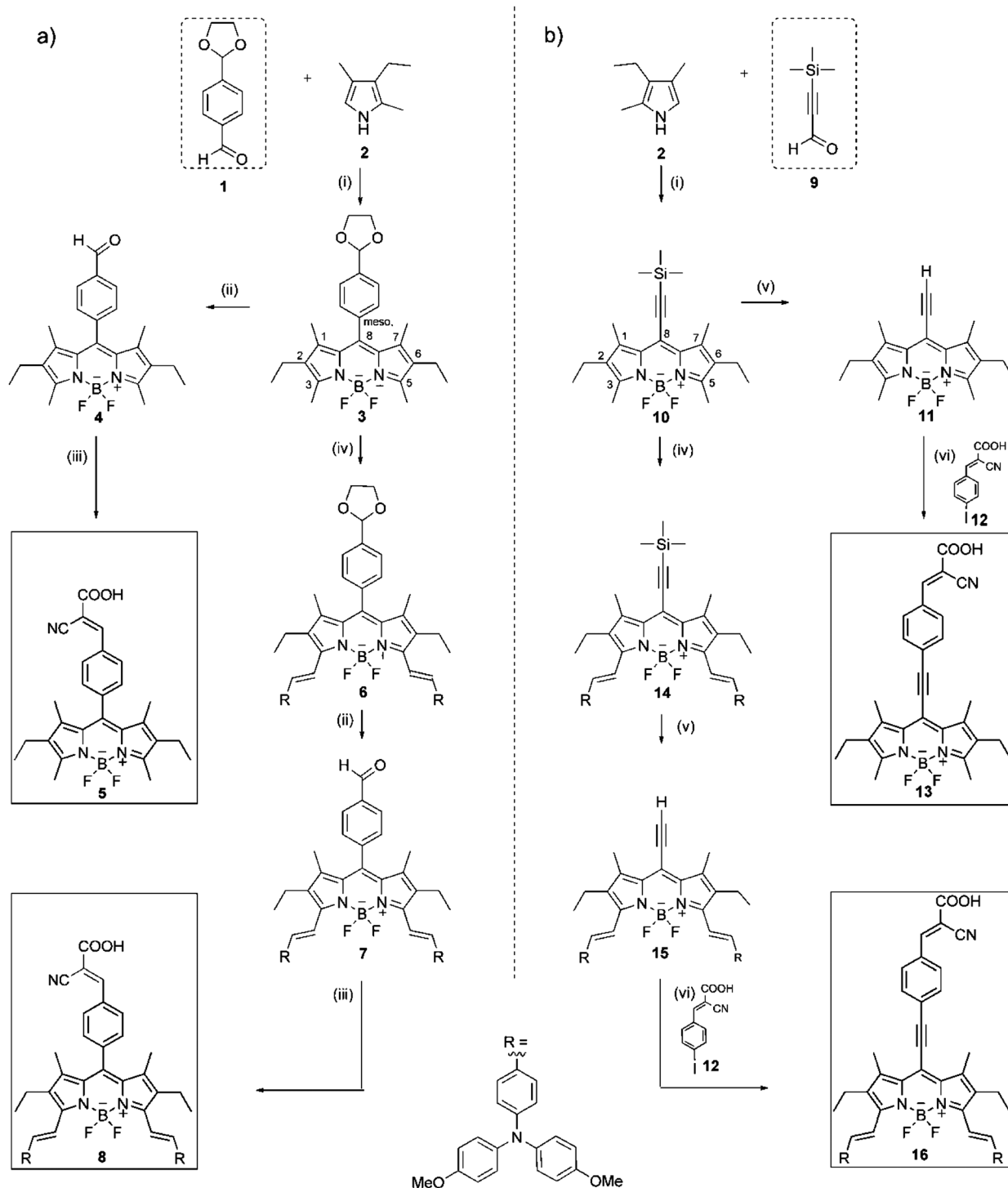
Scheme 1 Synthetic routes for the preparation of (a) the *meso*-phenyl BODIPYs (**5** and **8**) and (b) the *meso*-ethynylphenyl BODIPYs (**13** and **16**). (i) Trifluoroacetic acid, 2,3-dichloro-5,6-dicyano-1,4-benzoquinone, NEt₃, BF₃·OEt₂, in CH₂Cl₂, RT. (ii) 5% HCl$_{aq}$, in THF, RT. (iii) 2-Cyanoacetic acid, piperidine, in acetonitrile, reflux. (iv) 4-(Di(4-methoxyphenyl)amino)benzaldehyde, piperidine, glacial acetic acid, in benzene, reflux. (v) KF, in MeOH or MeOH : THF 1 : 1, RT. (vi) Pd(PPh₃)₄, CuI, NEt₃, in THF, RT.

ppm value for **3**. This is not due to the +M-effect of the phenyl group because it is not in conjugation with the BODIPY core. One possible influence affecting the shift is the spatial proximity between the electron density of the *meso*-phenyl ring and that of the methyl groups. However, the main effect influencing the shift is the ring current of the *meso*-phenyl group.

Consequently, the generated magnetic field weakens the applied one at the 1,7-methyl groups, which necessitates a higher external field. This equals a shift of the signal to lower ppm values. Therefore, it can be deduced that the *meso*-phenyl group does not influence the electron density at the 1,7-methyl groups by conjugation, but rather by the spatial proximity.
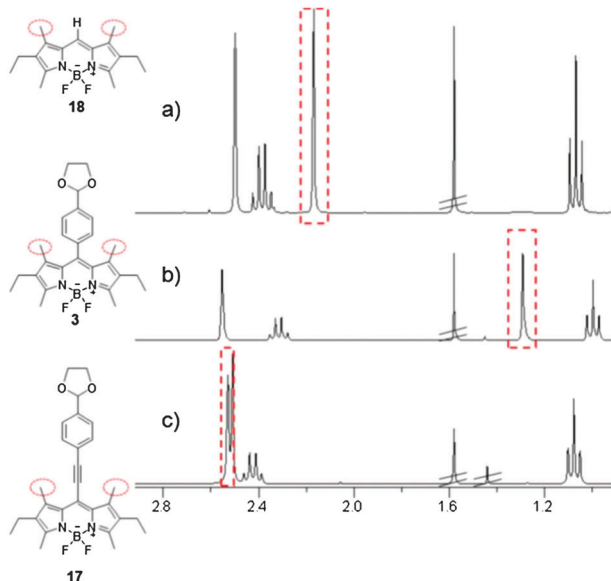
Fig. 1 Excerpts of the ^{1}H-NMR spectra of (a) the *meso*-proton BODIPY 1,3,5,7-tetramethyl-2,6-diethyl-4,4-difluoro-4-bora-3a,4a-diaza-s-indacene (**18**), (b) the *meso*-phenyl BODIPY (**3**) and (c) the corresponding *meso*-ethynylphenyl BODIPY (**17**). The red boxes mark the resonance signal attributed to the 1,7-methyl protons. (The signals at 1.56 and 1.44 ppm can be neglected because they arise from water and cyclohexane, respectively. The whole spectra are depicted in Fig. S7, ESI†.)

Further, the *meso*-phenyl group mainly affects the magnetic environment. In contrast, the *meso*-ethynyl bridge group is able to reduce the electron density at these positions through the conjugation. These observations are supported by the UV/vis measurements showing that the *meso*-ethynylphenyl BODIPY **17** causes a strong red shift due to the electron withdrawing ability of the *meso*-substituent whereas the corresponding *meso*-phenyl BODIPY **3** shows hardly any difference in the absorption relative to the *meso*-proton BODIPY **18** (Fig. S10, ESI†). However, the 3,5-methyl groups are only marginally influenced by the substituent at the *meso*-position.

Further, the stereochemistry of the vinyl bond between the BODIPY core and the donor group was investigated. On the basis of the ^{1}H-NMR spectra of **8** and **16** (Fig. S4 and S5, ESI†) the configuration can be clearly identified to be *trans* because the values for the vicinal $^3J_{H/H}$ couplings are 16.6 Hz and 16.4 Hz for **8** and **16**, respectively.

Finally, only the geometry of the 4-(2-carboxy-2-cyanovinyl)-phenyl anchoring unit of **5**, **8**, **13** and **16** required assignment. Here, the carboxyl group can be oriented either *cis* or *trans* relative to the phenyl group. Since this group was attached in a comparable manner for all end-products and for **12**, we used ^{13}C-NMR-analysis of **12** for the investigation of the orientation (see Fig. S9, ESI†). The double bond geometry of **12** could be unambiguously assigned as *trans*. This is also supported by the results of Karas *et al.*[22] who investigated the crystal structure of a very similar compound (2-cyano-3-(4-hydroxyphenyl)acrylic acid).

Optical properties

The electronic absorption spectra of **5**, **8**, **13** and **16** were recorded in solution and are depicted in Fig. 2a. Compound **5**
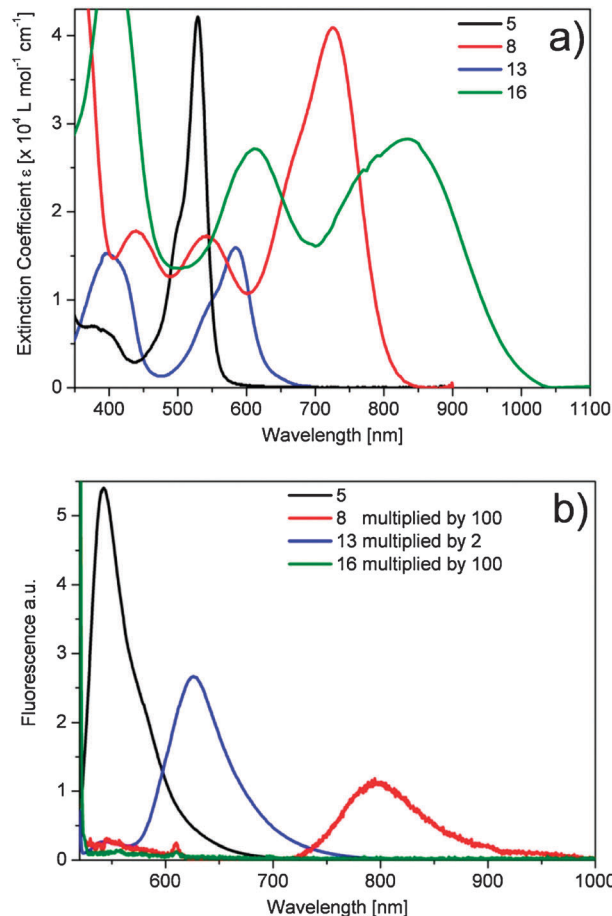
Fig. 2 (a) Electronic absorption spectra and (b) emission spectra of the BODIPYs **3** (in CH_2Cl_2), **8** (in CH_2Cl_2), **13** (in CH_2Cl_2 : THF 1 : 1) and **16** (in CH_2Cl_2) measured at a concentration in the range of 1×10^{-5} M.

shows the typical BODIPY absorption with the sharp S_0–S_1 transition at 530 nm and a high extinction coefficient ($\varepsilon = 4.21 \times 10^4$ M^{-1} cm^{-1}). Additionally, a shoulder appears at 500 nm which is attributed to the 0–1 vibrational transition. In comparison to that the S_0–S_1 transition of its *meso*-ethynylphenyl derivative (**13**) is red-shifted by 55 nm. The signal is broader and the extinction coefficient is reduced to 1.67×10^4 M^{-1} cm^{-1}. The 0–1 vibrational transition was detected at 542 nm. The reason for the reduced extinction coefficient of **13** compared to **5** is the larger spatial separation of the molecular orbitals involved in the transition. This is supported by DFT calculations (Fig. 3) which indicate an increased distance between HOMO and LUMO with the introduction of the *meso*-ethynyl unit. The larger distance lowers the transition probability. Thus, also the extinction coefficient is reduced. A further interesting feature of **13** is the absorption band at 397 nm. The extinction coefficient of this band is much higher for **13** than for **5**. We found that this band is associated with the *meso*-phenyl/ethynylphenyl unit. The pronounced band of **13** indicates that the electronic interaction between the BODIPY core and the *meso*-substituent can be increased by the *meso*-ethynyl group.
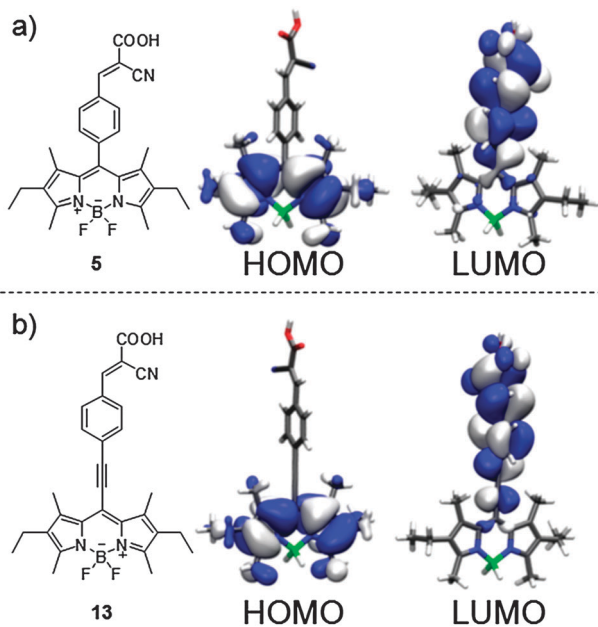
Fig. 3 Orbital maps of the HOMO and LUMO of (a) **5** and (b) **13**.

With the attachment of the MeOTPA donor groups, the absorption spectra of **5** and **13** experience a strong bathochromic shift. The absorption edge of **8** was detected at 840 nm and that of **16** at 1030 nm. The absorption maxima appear at 725 nm ($\varepsilon = 4.09 \times 10^4$ M^{-1} cm^{-1}) and 835 nm ($\varepsilon = 2.83 \times 10^4$ M^{-1} cm^{-1}) for **8** and **16**, respectively. These are excellent absorption ranges and extinction coefficients providing the possibility of improving the light harvesting of solar cells by using these dyes as sensitizers. It is important to note that the extinction coefficients of the MeOTPA-substituted BODIPYs are higher than 1×10^4 M^{-1} cm^{-1} over the whole visible spectrum up to 787 nm and 940 nm for **8** and **16**, respectively. This proves the excellent optical behaviour of BODIPYs carrying strong donor groups which is even more pronounced for *meso*-ethynylphenyl BODIPYs. The low energy bands of **8** and **16** can be attributed to intramolecular charge transfer.

To further investigate the influence of the ethynyl spacer and the donor substituents, steady-state emission measurements were done. Compared to **5**, the emission of **13** was remarkably reduced by the introduction of the ethynyl spacer (Fig. 2b). The fluorescence quantum yields in solution are 2.18 and 1.69% for **5** and **13**, respectively. For **8** and **16**, the fluorescence was too weak to determine the fluorescence quantum yield reliably. Additionally, the Stokes shift of **13** (Δ_{Stokes} = 42 nm) was more than thrice that of **5** (Δ_{Stokes} = 12 nm). The explanation for both observations lies within the different freedom of rotation of the phenyl rings.[16] The increased distance due to the ethynyl-bridge enables free rotation of the phenyl group around the axis given by the *meso*-spacer. In contrast, the *meso*-phenyl ring in **5** is restricted to an almost orthogonal position by the 1,7-dimethyl groups. Consequently, the emission probability of **13** is reduced *via* non-radiative decay due to the motion of the phenyl group.[16] Additionally, the

Stokes shift of **13** is increased due to stronger structural rearrangement. For the MeOTPA-substituted BODIPYs **8** and **16**, the fluorescence was very weak or even below the resolution of the spectrometer. This is attributed to a possible intramolecular charge transfer.

Electrochemical properties and DFT calculations

Cyclic voltammetry was used to examine the redox properties of the BODIPY dyes in solution. The energy levels of the final products are given in Table 1. Cyclic voltammograms of **5**, **8**, **13** and **16** and the deprotected counterparts **4**, **7**, **11**, and **15** as well as a table summarizing the redox values of all BODIPY derivatives are included in the ESI† (Fig. S11, S12, and Table S1).

In general, the BODIPY core and the donor substituent show a reversible behaviour, but on attaching the cyanocarboxylic acid group, the anodic and cathodic peak currents decrease. Therefore the peaks are less pronounced. In addition, a comparison of the calculated HOMO/LUMO energy levels of all compounds reveals two general trends: first, for all BODIPY compounds with methyl substituents, the only oxidation (denoted E_{OX1} = HOMO = -5.41 ± 0.03 eV) is unaffected by the substituent at the *meso*-position (see Table 1 and Table S1, ESI† for all compounds). This value of the E_{OX1} is thus assigned to the BODIPY core. It is also known from the literature that the HOMO of *meso*-phenyl BODIPY dyes without strong donor groups is delocalized over the BODIPY framework.[16,23] Secondly, with increasing electron withdrawing ability of the *meso*-substituent, the energy level of the LUMO is shifted to lower values. Consequently, the LUMO is dependent on the *meso*-substituent.

These findings are supported by DFT calculations on **5** (*meso*-phenyl) and **13** (*meso*-ethynylphenyl) (see Fig. 3). The LUMO of **5** is delocalized over the phenyl group and the anchoring group. For **13**, the LUMO is additionally distributed over the ethynyl-bridge. The delocalization of the LUMO over the *meso*-substituent is attributed to the strong electron withdrawing *para*-2-carboxy-2-cyanovinyl group. This is also in agreement with the literature.[16]

By the attachment of the MeOTPA-donor *via* a vinylic bond, the conjugated system is further extended. This can not only be seen in the absorption, but also in the cyclic voltammetry experiments.

The cyclic voltammograms of all MeOTPA-substituted BODIPYs show three reversible oxidation signals (Fig. S11 and S12, ESI†).

Table 1 Summary of the energy levels calculated from cyclic voltammetry experiments measured at 50 mV s^{-1} in CH$_2$Cl$_2$ with 0.1 M tetrabutylammonium hexafluorophosphate using ferrocene as reference

Compound	E_{OX1}[a] [eV]	E_{OX2} [eV]	E_{OX3} [eV]	E_{LUMO}[b] [eV]
5	-5.40	—	—	-3.18
13	-5.44	—	—	-3.48
8	-4.84	-4.97	-5.42	-3.28
16	-4.84	-4.98	-5.43	-3.59

[a] E_{OX1} is considered as the HOMO energy value. [b] The LUMO levels were calculated from the optical band gap.

The one at -5.4 eV arising from the BODIPY core as discussed above and the two lower lying peaks (-4.84 ± 0.01 eV, -4.97 ± 0.01 eV) originate from the MeOTPA group. In fact, for non-conjugated systems, only one oxidation peak would be expected for the MeOTPA unit. However, we detected two reversible oxidations for the MeOTPA substituent. This is due to the conjugation of the MeOTPA-moieties through the BODIPY core. The oxidation of one donor unit influences the electronic surrounding of the second one due to the conjugation.[24]

A further characteristic of the BODIPY derivatives is their stability against repeated oxidation and reduction cycles. Even, the MeOTPA-substituted BODIPYs were stable during repeated electrochemical measurements because the *para*-methoxy groups of the donors inhibit radical coupling of the triphenylamines.

In a nutshell, the BODIPYs are redox stable, their LUMO level can be tuned by the *meso*-substituent and the HOMO level can be adjusted by the donor groups.

Photocurrent generation

To elucidate the potential of BODIPYs **5**, **8**, **13** and **16** as light harvesters, we prepared solid-state dye-sensitized solar cells with these sensitizers and measured the incident photon-to-current conversion efficiency (IPCE) for each sample (Fig. 4). The final IPCE values depend on the optimization of device structure and adaptation of HOMO/LUMO values of the hole transport material used. Here we tested the applicability of the dyes using a reference hole transport material, spiro-OMeTAD. In general, both **8** and **16** show broad photoaction spectra. A comparison between the performance of **5** and **13** shows that **13** carrying a *meso*-ethynyl substituent contributes to the current generation over a much broader region. In accordance with the absorption measurements, **5** generates current up to 600 nm, whereas **13** contributes up to 700 nm. Due to a mismatch in the energy levels of the MeOTPA-substituted BODIPYs **8** and **16** ($E_{\mathrm{OX1}} = -4.84$ eV) relative to the hole transport material spiro-OMeTAD ($E_{\mathrm{OX1}} = -4.91$ eV),[25] the absolute IPCE values for **8** and **16** are low. Nevertheless, the IPCE measurements clearly show that BODIPYs **8** and **16** contribute to the current generation

over their entire absorption region; **8** and **16** generating photo-current up to 900 nm and 1000 nm, respectively. All the sensitizers provide a high potential for improvement by further optimization, *e.g.* by selecting suitable hole transport materials, tuning the thickness to match recombination and transport, *etc.*

Conclusions

We reported the tailor-made synthesis of novel BODIPY sensitizers capable of light harvesting and energy conversion in a broad range. The synthesis included the variation of the *meso*-substituent (phenyl *vs.* ethynylphenyl) and the substituents at positions 3 and 5 (methyl *vs.* MeOTPA).

Investigations of the optical properties of **5**, **8**, **13** and **16** showed that the introduction of the ethynyl-bridge between the BODIPY core and the phenyl ring causes a strong bathochromic shift of the absorption (**5** *vs.* **13** and **8** *vs.* **16**). Further, a more than panchromatic behaviour resulted for both the *meso*-phenyl and the *meso*-ethynylphenyl BODIPYs as a consequence of the attachment of MeOTPA-donor groups (**8** and **16**). In particular, **8** and **16** provide molar extinction coefficients higher than 1×10^4 M^{-1} cm^{-1} over the whole UV/vis region and up to the near-IR part. **16** absorbs up to 1030 nm making this dye particularly interesting as sensitizers for solar cells.

Furthermore, cyclic voltammetry experiments showed that the HOMO level of the BODIPY depends solely on the donor unit regardless of the substituents at the *meso*-position. The measured HOMO levels were -5.41 ± 0.03 eV and -4.84 ± 0.01 eV for BODIPYs with methyl and MeOTPA donor groups, respectively. In contrast, the LUMO level depends on the *meso*-substituent. Electron withdrawing substituents like the ethynyl group shift the level to lower values. The HOMO/LUMO distributions are further supported by DFT calculations.

IPCE measurements on solid-state dye-sensitized solar cells sensitized with BODIPYs **5**, **8**, **13** and **16** showed that the BODIPYs can contribute to the photocurrent generation over the entire absorption region.

Experimental

General

^{1}H-NMR spectra were recorded on a Bruker Avance 300 spectrometer at a transmitter frequency of 300 MHz. ^{1}H–^{13}C coupled NMR spectra were recorded at a frequency of 125 MHz. The spectra were calibrated relative to the chemical shift of the respective solvent residual signal. The chemical shifts (δ) are given in ppm and the coupling constants (J) in Hz. UV/vis spectra were recorded in CH$_2$Cl$_2$ (or in THF : CH$_2$Cl$_2$ 1 : 1 for **13**) on a Hitachi U-3000 spectrophotometer and in a Bentham DTR6 integrating sphere at a concentration in the range of 1×10^{-5} M. The extinction coefficients (ε) were calculated according to the Beer–Lambert law. Steady-state fluorescence measurements were performed on a JASCO Spectrofluorometer ST-8600. The slit width was 5 nm for excitation and emission. The photomultiplier voltage was 800 V. For the determination of the fluorescence quantum yields, the area for the corrected
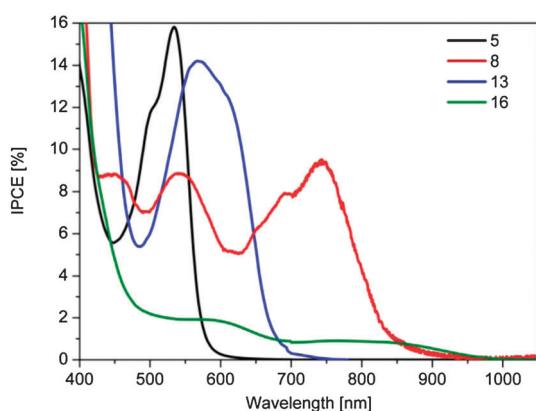
Fig. 4 IPCE-curves of solid-state dye-sensitized solar cells sensitized with BODIPYs **5**, **8**, **13** and **16**.

emission spectra was divided by the corrected area of the absorbed light peak. The samples were excited at a wavelength 30 nm blue-shifted relative to the longest wavelength absorption maximum. Cyclic voltammetry was carried out under moisture- and oxygen-free conditions using a standard three-electrode assembly connected to a potentiostat (model 263A, EG&G Princeton Applied Research) at a scanning rate of 50 mV s^{-1}. A Pt milli-electrode (model G0228, AMETEK Advanced Measurement Technology) was used as a working electrode. A platinum wire in the respective solvent plus conducting salt (tetrabutylammonium hexafluorophosphate, 0.1 M) was used as a counter electrode. The quasi-reference electrode consisted of an Ag-wire in an AgNO$_3$/acetonitrile solution (0.1 M). Each measurement was calibrated with the internal standard ferrocene/ferrocenium. The energy levels were determined using the empirical relation $E_{HOMO \text{ or } LUMO} = [-e(E^{1/2}_{(x \text{ } vs. \text{Ag/AgNO}_3)} - E^{1/2}_{(Fc/Fc+ vs. \text{Ag/AgNO}_3)})] -$ 4.80 eV. Molecular geometries, energy levels and orbitals were calculated from density functional theory at the B3LYP/cc-pVTZ level using the TURBOMOLE program package.[26] Solid-state dye-sensitized solar cells were prepared according to a method reported elsewhere.[27] IPCE spectra were recorded using a PVE300 photovoltaic device characterization system from Bentham.

Synthesis

4-(1,3-Dioxolan-2-yl)benzaldehyde (1),[28] 8-[4-(1,3-dioxolan-2-yl)-phenyl]-1,3,5,7-tetramethyl-2,6-diethyl-4,4-difluoro-4-bora-3a,4a-diaza-s-indacene (3),[14] 2-(4-iodophenyl)-1,3-dioxolane[29] and 4-(di(4-methoxyphenyl)amino)benzaldehyde[30] were prepared according to standard procedures. 1,3,5,7-Tetramethyl-2,6-diethyl-4,4-difluoro-4-bora-3a,4a-diaza-s-indacene (18) was isolated during the synthesis of 10. Compounds 10 and 11 can also be synthesised according to ref. 31. 3-Ethyl-2,4-dimethyl-1H-pyrrole and 3-trimethylsilylpropanal are commercially available. The syntheses of all other compounds are described below.

8-(4-Formylphenyl)-1,3,5,7-tetramethyl-2,6-diethyl-4,4-difluoro-4-bora-3a,4a-diaza-s-indacene (4). 3 (200.0 mg, 0.463 mmol) is dissolved in THF (50 mL) and 5% HCl$_{aq}$ (10 mL) is added. The solution is stirred for 3.5 h. Then CH$_2$Cl$_2$ (100 mL) is added and the solution is washed with diluted NaHCO$_{3aq}$ (50 mL) and water (4 × 80 mL) until neutrality. The organic phase is dried over Na$_2$SO$_4$, filtered and the solvent is removed under vacuum to yield the pure product. Yield: 189 mg (red solid), 100%. λ_{max}(DCM)/nm = 528 (ε/M^{-1} cm^{-1} = 58 300), 500sh (20 481). FT-IR (ATR): ν_{max}/cm^{-1} = 3361 (w), 2965 (m), 1701 (m), 1536 (s), 1470 (m), 1405 (m), 1317 (s), 1262 (m), 1184 (s), 1052 (m), 974 (s), 798 (m). ^{1}H-NMR (300 MHz, CDCl$_3$): δ/ppm = 1.00 (t, $^3J_{1H/1H}$ = 7.53 Hz, 6H, 2/6-CH$_2$CH$_3$), 1.27 (s, 6H, 1/7-CH$_3$), 2.32 (q, $^3J_{1H/1H}$ = 7.59 Hz, 4H, 2/6-CH$_2$CH$_3$), 2.56 (s, 6H, 3/5-CH$_3$), 7.53 (d, $^3J_{1H/1H}$ = 8.04 Hz, 2H, 8-H_{ar}), 8.04 (d, $^3J_{1H/1H}$ = 8.25 Hz, 2H, 8-H_{ar}), 10.14 (s, 1H, COH).

8-[4-(2-Carboxy-2-cyanovinyl)phenyl]-1,3,5,7-tetramethyl-2,6-diethyl-4,4-difluoro-4-bora-3a,4a-diaza-s-indacene (5). 2-Cyano-acetic acid (218.7 mg, 2.572 mmol, 7 eq.) and 4 (150.0 mg, 0.367 mmol, 1 eq.) are dissolved in dry acetonitrile (35 mL) and piperidine (50 µL) is added. Then, the solution is heated to reflux for 3 h. The solvent is removed and the residue is

dissolved in CH$_2$Cl$_2$ washed with water (4 × 80 mL), dried over Na$_2$SO$_4$ and is concentrated. The raw product is purified by column chromatography with toluene : methanol 5 : 1 as eluent. Yield after freeze-drying from 1,4-dioxane: 158 mg (red-orange solid, R_f (SiO$_2$; toluene : methanol 5 : 1) = 0.20), 90%. λ_{max}(DCM)/nm = 530 (ε/M^{-1} cm^{-1} = 42 137), 500sh (18 610), 381 (6951). FT-IR (ATR): ν_{max}/cm^{-1} = 3464 (br), 2964 (w), 2223 (w) 1629 (w), 1539 (s), 1629 (m), 1470 (m), 1393 (m), 1187 (s), 1057 (m), 977 (s), 708 (m). ^{1}H-NMR (300 MHz, DMSO-d$_6$): δ/ppm = 0.94 (t, $^3J_{1H/1H}$ = 7.02 Hz, 6H, 2/6-CH$_2$CH$_3$), 1.28 (s, 6H, 1/7-CH$_3$), 2.27 (q, $^3J_{1H/1H}$ = 6.99 Hz, 4H, 2/6-CH$_2$CH$_3$), 2.44 (s, 6H, 3/5-CH$_3$), 7.57 (d, $^3J_{1H/1H}$ = 8.16 Hz, 2H, 8-H_{ar}), 8.14 (d, $^3J_{1H/1H}$ = 8.07 Hz, 2H, 8-H_{ar}), 8.27 (s, 1H, Ph–CH=C(COOH)(CN)).

8-[4-(1,3-Dioxolan-2-yl)phenyl]-1,7-dimethyl-3,5-di[4-(di-(p-methoxyphenyl)-amino)styryl]-2,6-diethyl-4,4-difluoro-4-bora-3a,4a-diaza-s-indacene (6). To a solution of 3 (100.0 mg, 0.221 mmol, 1 eq.) and 4-(di(4-methoxyphenyl)amino)-benzaldehyde (221.1 mg, 0.663 mmol, 3 eq.) in benzene (20 mL), piperidine (0.3 mL) and glacial acetic acid (0.25 mL) were added. After heating the solution to reflux over a glass frit containing molecular sieve (4 Å) for 11 h, the solvent is removed and the raw product is purified by column chromatography using cyclohexane : ethyl acetate 2 : 1 as eluent. Yield: 77 mg (green-black solid, R_f (SiO$_2$; cyclohexane : ethyl acetate 2 : 1) = 0.30), 32%. λ_{max}(DCM)/nm = 715 (ε/M^{-1} cm^{-1} = 56 444), 534 (20 179), 437 (21 739), 358 (50 498). FT-IR (ATR): ν_{max}/cm^{-1} = 2962 (w), 1587 (m), 1503 (s), 1441 (m), 1242 (s), 1174 (s), 1028 (m), 819 (m). ^{1}H-NMR (300 MHz, CDCl$_3$): δ/ppm = 1.15 (t, $^3J_{1H/1H}$ = 7.50 Hz, 6H, 2/6-CH$_2$CH$_3$), 1.32 (s, 6H, 1/7-CH$_3$); 2.61 (q, $^3J_{1H/1H}$ = 7.47 Hz, 4H, 2/6-CH$_2$CH$_3$), 3.83 (s, 12H, OMe), 4.09–4.26 (m, 4H, O–CH$_2$CH$_2$–O), 5.90 (s, 1H, Ph–CH), 6.86 (d, $^3J_{1H/1H}$ = 8.97 Hz, 8H, 3/5-H_{ar}), 6.93 (d, $^3J_{1H/1H}$ = 8.70 Hz, 4H, 3/5-H_{ar}), 7.10 (d, $^3J_{1H/1H}$ = 8.94 Hz, 8H, 3/5-H_{ar}), 7.19 (d, $^3J_{1H/1H}$ = 16.71 Hz, 2H; 3/5CH=CH), 7.36 (d, $^3J_{1H/1H}$ = 8.07 Hz, 2H, 8-H_{ar}), 7.42 (d, $^3J_{1H/1H}$ = 8.73 Hz, 4H, 3/5-H_{ar}), 7.64 (d + d, $^3J_{1H/1H}$ = 8.22 Hz, 2H + 2H, 3/5CH=CH + 8-H_{ar}).

8-(4-Formylphenyl)-1,7-dimethyl-3,5-di[4-(di(p-methoxy-phenyl)-amino)-styryl]-2,6-diethyl-4,4-difluoro-4-bora-3a,4a-diaza-s-indacene (7). 6 (100.0 mg, 0.092 mmol) is dissolved in THF (40 mL) and 5% HCl$_{aq}$ (5 mL) is added. The solution is stirred overnight. Then CH$_2$Cl$_2$ (100 mL) is added and the solution is washed with diluted NaHCO$_{3aq}$ (50 mL) and water (4 × 100 mL) until neutrality. The organic phase is dried over Na$_2$SO$_4$, filtered and the solvent is removed under vacuum to yield the pure product. Yield: 95 mg (green-black solid), 99%. λ_{max}(DCM)/nm = 723 (ε/M^{-1} cm^{-1} = 55 388), 545 (21 318), 440 (21 318), 360 (51 403). FT-IR (ATR): ν_{max}/cm^{-1} = 2961 (w), 1705 (w), 1590 (m), 1502 (s), 1440 (m), 1240 (m), 1171 (m), 1035 (m), 822 (m). ^{1}H-NMR (300 MHz, CDCl$_3$): δ/ppm = 1.16 (t, $^3J_{1H/1H}$ = 7.32 Hz, 6H, 2/6-CH$_2$CH$_3$), 1.30 (s, 6H, 1/7-CH$_3$), 2.61 (q, $^3J_{1H/1H}$ = 7.35 Hz, 4H; 2/6-CH$_2$CH$_3$), 3.83 (s, 12H, OMe), 6.87 (d, $^3J_{1H/1H}$ = 8.94 Hz, 8H, 3/5-H_{ar}), 6.93 (d, $^3J_{1H/1H}$ = 8.67 Hz, 4H, 3/5-H_{ar}), 7.10 (d, $^3J_{1H/1H}$ = 8.94 Hz, 8H, 3/5-H_{ar}), 7.20 (d, $^3J_{1H/1H}$ = 16.66 Hz, 2H, 3/5CH=CH), 7.45 (d, $^3J_{1H/1H}$ = 8.67 Hz, 4H, 3/5-H_{ar}), 7.55 (d, $^3J_{1H/1H}$ = 8.01 Hz, 2H, 8-H_{ar}), 7.64 (d, $^3J_{1H/1H}$ = 16.54 Hz, 2H, 3/5CH=CH), 8.04 (d, $^3J_{1H/1H}$ = 8.07 Hz, 2H, 8-H_{ar}), 10.15 (s, 1H, COH).

8-[4-(2-Carboxy-2-cyanovinyl)phenyl]-1,7-dimethyl-3,5-di-[4-(di(*p*-methoxy-phenyl)amino)styryl]-2,6-diethyl-4,4-difluoro-4-bora-3a,4a-diaza-*s*-indacene (8). 2-Cyanoacetic acid (65.6 mg, 0.772 mmol, 7 eq.) and **7** (114.3 mg, 0.110 mmol, 1 eq.) are dissolved in dry acetonitrile (35 mL) and three drops of piperidine are added. Then, the solution is heated to reflux for 5 h. The solvent is removed and the residue is dissolved in CH$_2$Cl$_2$, washed with water (4 × 80 mL), dried over Na$_2$SO$_4$ and the solvent is removed under vacuum. The raw product is purified by column chromatography with CH$_2$Cl$_2$: methanol 15 : 1 as eluent. Yield after freeze-drying from 1,4-dioxane: 72 mg (brown-black solid, R_f (SiO$_2$; CH$_2$Cl$_2$: methanol 15 : 1) = 0.45), 59%. λ_{max}(DCM)/nm = 725 (ε/M^{-1} cm^{-1} = 40 889), 543 (17 258), 439 (17 846), 358 (48 342). FT-IR (ATR): ν_{max}/cm^{-1} = 3405 (br), 2963 (w), 2222 (w), 1593 (m), 1503 (s), 1440 (m), 1332 (m), 1241 (s), 1171 (s), 1034 (m), 823 (m). ^{1}H-NMR (300 MHz, DMSO-d$_6$): δ/ppm = 1.07 (t, $^3J_{1H/1H}$ = 7.26 Hz, 6H, 2/6-CH$_2$CH$_3$), 1.31 (s, 6H; 1/7-CH$_3$), 2.58 (q, $^3J_{1H/1H}$ = 6.75 Hz, 4H; 2/6-CH$_2$CH$_3$), 3.76 (s, 12H, OMe), 6.78 (d, $^3J_{1H/1H}$ = 8.73 Hz, 4H, 3/5-H$_{ar}$), 6.93 (d, $^3J_{1H/1H}$ = 9.00 Hz, 8H, 3/5-H$_{ar}$), 7.07 (d, $^3J_{1H/1H}$ = 8.94 Hz, 8H, 3/5-H$_{ar}$), 7.21 (d, $^3J_{1H/1H}$ = 16.59 Hz, 2H, 3/5CH=CH), 7.41 (d, $^3J_{1H/1H}$ = 16.65 Hz, 2H, + d, 4H, $^3J_{1H/1H}$ = 8.85 Hz, 3/5CH=CH + 3/5-H$_{ar}$), 7.56 (d, $^3J_{1H/1H}$ = 8.22 Hz, 2H, 8-H$_{ar}$), 8.10 (d, $^3J_{1H/1H}$ = 8.37 Hz, 2H, 8-H$_{ar}$), 8.16 (s, 1H, Ph–CH=C(COOH)(CN)).

8-[(Trimethylsilyl)ethynyl]-1,3,5,7-tetramethyl-2,6-diethyl-4,4-difluoro-4-bora-3a,4a-diaza-*s*-indacene (10). Under dry conditions, 3-ethyl-2,4-dimethyl-1*H*-pyrrole (13.664 g, 110.909 mmol, 2 eq.) is dissolved in dry CH$_2$Cl$_2$ (300 mL), cooled to −5 °C and degassed with argon for 30 min. Then 3-trimethylsilylpropanal (7.000 g, 55.454 mmol, 1 eq.) and one drop of trifluoroacetic acid are added. The solution instantly becomes orange, and changes the colour firstly to red and then to deep violet. After 1 h 2,3-dichloro-5,6-dicyano-1,4-benzoquinone (12.588 g, 55.454 mmol, 1 eq.) is added at RT and stirring is continued overnight. NEt$_3$ (46.4 mL, 332.726 mmol, 6 eq.) and 30 min later BF$_3$·OEt$_2$ (55.7 mL, 443.635 mmol, 8 eq.) are added slowly. Stirring is continued for further 3 h. Then the solvent is removed under reduced pressure and the raw product is purified by column chromatography using cyclohexane : ethyl acetate 13 : 1 as eluent. Yield: 9.66 g (pink-black solid, R_f (SiO$_2$; cyclohexane : ethyl acetate 13 : 1) = 0.49), 44%. λ_{max}(DCM)/nm = 574 (ε/M^{-1} cm^{-1} = 49 206), 537sh (22 374), 360 (12 028), 274 (23 552). FT-IR (ATR): ν_{max}/cm^{-1} = 2963 (w), 1533 (m), 1455 (m), 1311 (m), 1181 (m), 1072 (m), 971 (m), 843 (m), 751 (m). ^{1}H-NMR (300 MHz, CDCl$_3$): δ/ppm = 0.31 (s, 9H, Si(CH)$_3$), 1.06 (t, $^3J_{1H/1H}$ = 7.53 Hz, 6H, 2/6-CH$_2$CH$_3$), 2.41 (s, 6H, 1/7-CH$_3$), 2.41 (q, $^3J_{1H/1H}$ = 7.56 Hz, 4H, 2/6-CH$_2$CH$_3$), 2.51 (s, 6H; 3/5-CH$_3$).

8-Ethynyl-1,3,5,7-tetramethyl-2,6-diethyl-4,4-difluoro-4-bora-3a,4a-diaza-*s*-indacene (11). **10** (400.0 mg, 0.999 mmol, 1 eq.) is dissolved in methanol (80 mL), KF (290.2 mg, 4.995 mmol, 5 eq.) is added and the reaction solution is stirred for 1.5 h at RT. After full consumption of the starting material, 1% CH$_3$COOH$_{aq}$ (50 mL) is added. Then, CH$_2$Cl$_2$ (150 mL) is added and the organic layer is washed with water (4 × 80 mL) until neutrality. It is dried over Na$_2$SO$_4$ and the solvent is removed under vacuum. Yield: 327 mg (pink-black solid), 100%.

λ_{max}(DCM)/nm = 572 (ε/M^{-1} cm^{-1} = 59 850), 534sh (26 194), 352 (8205), 265 (21 775) FT-IR (ATR): ν_{max}/cm^{-1} = 3263 (m), 2960 (m), 2107 (m), 1535 (m), 1456 (m), 1394 (m), 1311 (m), 1264 (m), 1187 (m), 1041 (s), 970 (s), 754 (m). ^{1}H-NMR (300 MHz, CDCl$_3$): δ/ppm = 1.07 (t, $^3J_{1H/1H}$ = 7.53 Hz, 6H, 2/6-CH$_2$CH$_3$), 2.41 (s, 6H, 1/7-CH$_3$), 2.41 (q, $^3J_{1H/1H}$ = 7.56 Hz, 4H, 2/6-CH$_2$CH$_3$), 2.52 (s, 6H, 3/5-CH$_3$), 3.89 (s, 1H, ≡H).

2-Cyano-3-(4-iodophenyl)acrylic acid (12). Under dry conditions, 4-iodobenzaldehyde (7.400 g, 31.894 mmol, 1 eq.) is dissolved in benzene (90 mL). Piperidine (0.90 mL), glacial acetic acid (0.75 mL) and 2-cyanoacetic acid (18.990 g, 0.223 mol, 7 eq.) are added. The solution is heated to reflux over a glass frit containing molecular sieve (4 Å) for 40 h. Then, the solvent is removed and the raw product is purified by repetitive recrystallisation from CH$_2$Cl$_2$. Yield: 5.03 g (white solid), 53%. FT-IR (ATR): ν_{max}/cm^{-1} = 3312 (br), 2222 (m), 1623 (s), 1578 (s), 1481 (m), 1387 (s), 1187 (w), 1058 (m), 1005 (s), 817 (s), 781 (m). ^{1}H-NMR (300 MHz, DMSO-d$_6$): δ/ppm = 7.79 (d, $^3J_{1H/1H}$ = 8.52 Hz, 2H, 2-H$_{ar}$), 7.98 (d, $^3J_{1H/1H}$ = 8.46 Hz, 2H, 3-H$_{ar}$), 8.30 (s, 1H, Ph–CH=C(COOH)(CN)), 14.04 (s (broad), 1H, COOH). ^{13}C-NMR (125 MHz, DMSO-d$_6$): δ = 163.19 (d, $^3J_{1H/13C}$ = 6.7 Hz, COOH), 153.46 (d, $^1J_{1H/13C}$ = 162.2 Hz, CH=C(COOH)(CN)), 138.29 (d, $^1J_{1H/13C}$ = 167.6 Hz, 3/5-C$_{ar}$), 132.06 (d, $^1J_{1H/13C}$ = 162.8 Hz, 2/6-C$_{ar}$), 130.91 (s, 1-C$_{ar}$), 115.97 (d, $^3J_{1H/13C}$ = 13.9 Hz, CN), 104.43 (s, CH=C(COOH)(CN)), 101.50 (s, 4-C$_{ar}$).

8-[[4-(2-Carboxy-2-cyanovinyl)phenyl)ethynyl]-1,3,5,7-tetramethyl-2,6-diethyl-4,4-difluoro-4-bora-3a,4a-diaza-*s*-indacene (13). Under dry and oxygen-free conditions, **12** (820.0 mg, 2.742 mmol, 3 eq.), Pd(PPh$_3$)$_4$ (63.4 mg, 0.055 mmol, 0.06 eq.), CuI (6.9 mg, 0.036 mmol, 0.04 eq.) and NEt$_3$ (0.60 mL, 4.296 mmol, 4.7 eq.) are dissolved in dry THF (13 mL). Then, **11** (300.0 mg, 0.914 mmol, 1 eq.) is dissolved in dry THF (20 mL) and added dropwise over 3 h at RT to the reaction solution. After further 60 min stirring at RT, the solvent is removed. The residue is dissolved in CHCl$_3$ and washed with water (4 × 100 mL). The organic fraction is dried over Na$_2$SO$_4$ and filtered. After removal of the solvent, the raw product is purified by column chromatography with cyclohexane : ethyl acetate 2 : 1 + 1% of glacial acetic acid, then the solvent is changed to CH$_2$Cl$_2$ followed by a change to CH$_2$Cl$_2$: methanol 20 : 1 with a gradient to 10 : 1. Yield: 218 mg (purple-black solid, R_f (SiO$_2$; CH$_2$Cl$_2$: methanol 10 : 1) = 0.50), 48%. λ_{max}(DCM : THF 1 : 1)/nm = 585 (ε/M^{-1} cm^{-1} = 16 708), 542sh (9628), 397 (16 047), 279 (21 144). FT-IR (ATR): ν_{max}/cm^{-1} = 3403 (br), 2963 (w), 2214 (w), 1631 (w), 1539 (m), 1472 (m), 1392 (m), 1321 (m), 1194 (s), 1043 (m), 977 (s), 801 (m), 754 (m). ^{1}H-NMR (300 MHz, DMF-d$_7$): δ/ppm = 1.07 (t, $^3J_{1H/1H}$ = 7.38 Hz, 6H, 2/6-CH$_2$CH$_3$), 2.46 (q, $^3J_{1H/1H}$ = 7.53 Hz, 4H, 2/6-CH$_2$CH$_3$), 2.53 (s, 6H, 3/5-CH$_3$), 2.58 (s, 6H, 1/7-CH$_3$), 7.87 (d, $^3J_{1H/1H}$ = 8.34 Hz, 2H, 8-H$_{ar}$), 8.09 (d, $^3J_{1H/1H}$ = 8.28 Hz, 2H, 8-H$_{ar}$), 8.29 (s, 1H, Ph–CH=C(COOH)(CN)).

8-[(Trimethylsilyl)ethynyl]-1,7-dimethyl-3,5-di[4-(di(*p*-methoxy-phenyl)-amino)styryl]-2,6-diethyl-4,4-difluoro-4-bora-3a,4a-diaza-*s*-indacene (14). Under dry conditions, 4-(di(4-methoxyphenyl)-amino)benzaldehyde (1.873 g, 5.620 mmol, 3 eq.) is dissolved in dry benzene (40 mL). Piperidine (0.30 mL), glacial acetic acid (0.25 mL) and finally **10** (750.0 mg, 1.873 mmol, 1 eq.) are added.

The reaction solution is heated to reflux over a glass frit containing molecular sieve (4 Å) to remove the formed water. After complete consumption of the staring material (21 h), the solvent is removed and the raw product is purified by column chromatography using CH_2Cl_2 : hexane 9 : 1 as eluent. Yield: 800 mg (blue-black solid, R_f (SiO$_2$; CH_2Cl_2 : hexane 9 : 1) = 0.23), 41%. λ_{max}(DCM)/nm = 784 (ε/M^{-1} cm^{-1} = 62 815), 582 (28 346), 465 (17 482), 381 (60 544). FT-IR (ATR): ν_{max}/cm^{-1} = 2959 (w), 2148 (w), 1587 (m), 1497 (s), 1440 (m), 1237 (m), 1161 (m), 1029 (m), 818 (m). ^{1}H-NMR (300 MHz, benzene-d$_6$): δ/ppm = 0.22 (s, 9H, Si(CH_3)), 1.07 (t, $^3J_{1H/1H}$ = 7.29 Hz, 6H, 2/6-CH$_2$CH_3), 2.36 (s, 6H, 1/7-CH_3), 2.55 (q, $^3J_{1H/1H}$ = 7.38 Hz, 4H, 2/6-CH_2CH$_3$), 3.37 (s, 12H, OMe), 6.75 (d, $^3J_{1H/1H}$ = 9.00 Hz, 8H, 3/5-H_{ar}), 6.84 (d, $^3J_{1H/1H}$ = 8.70 Hz, 4H, 3/5-H_{ar}), 7.04 (d, $^3J_{1H/1H}$ = 8.94 Hz, 8H, 3/5-H_{ar}), 7.38 (d, $^3J_{1H/1H}$ = 16.66 Hz, 2H, 3/5CH=CH), 7.48 (d, $^3J_{1H/1H}$ = 8.73 Hz, 4H, 3/5-H_{ar}), 8.42 (d, $^3J_{1H/1H}$ = 16.51 Hz, 2H, 3/5CH=CH).

8-Ethynyl-1,7-dimethyl-3,5-di[4-(di(p-methoxyphenyl)-amino)-styryl]-2,6-diethyl-4,4-difluoro-4-bora-3a,4a-diaza-s-indacene (15). 14 (790.0 mg, 0.766 mmol, 1 eq.) is dissolved in THF : methanol 1 : 1 (80 mL of each), KF (222.6 mg, 3.831 mmol, 5 eq.) is added and the reaction solution is stirred for 30 min at RT. Then 1% CH_3COOH_{aq} (50 mL) and CH_2Cl_2 (150 mL) are added. The organic layer is washed with water (4 × 100 mL) until neutrality, dried over Na$_2$SO$_4$, filtered and the solvent is removed under vacuum. Yield: 710 mg (blue-black solid), 97%. λ_{max}(DCM)/nm = 781 (ε/M^{-1} cm^{-1} = 49 415), 580 (22 659), 461 (16 994), 372 (49 970). FT-IR (ATR): ν_{max}/cm^{-1} = 3274 (w), 2961 (w), 1587 (m), 1500 (s), 1240 (m), 1171 (m), 1033 (m), 821 (m). ^{1}H-NMR (300 MHz, THF-d$_8$): δ/ppm = 1.24 (t, $^3J_{1H/1H}$ = 7.17 Hz, 6H, 2/6-CH$_2$CH_3), 2.53 (s, 6H, 1/7-CH_3), 2.78 (q, $^3J_{1H/1H}$ = 7.44 Hz, 4H, 2/6-CH_2CH$_3$), 3.80 (s, 12H, OMe), 4.69 (s, 1H; ≡H), 6.88 (d + d, $^3J_{1H/1H}$ = 7.02 Hz, 4H + 8H, 3/5-H_{ar}), 7.08 (d, $^3J_{1H/1H}$ = 8.94 Hz, 8H, 3/5-H_{ar}), 7.28 (d, $^3J_{1H/1H}$ = 16.74 Hz, 2H, 3/5CH=CH), 7.41 (d, $^3J_{1H/1H}$ = 8.73 Hz, 4H, 3/5-H_{ar}), 7.63 (d, $^3J_{1H/1H}$ = 16.60 Hz, 2H, 3/5CH=CH).

8-[(4-(2-Carboxy-2-cyanovinyl)phenyl)ethynyl]-1,7-dimethyl-3,5-di[4-(di(p-methoxyphenyl)amino)styryl]-2,6-diethyl-4,4-difluoro-4-bora-3a,4a-diaza-s-indacene (16). Under dry and oxygen-free conditions, 12 (280.1 mg, 0.939 mmol, 3 eq.), Pd(PPh$_3$)$_4$ (21.7 mg, 0.019 mmol, 0.06 eq.), CuI (2.4 mg, 0.013 mmol, 0.04 eq.) and NEt$_3$ (0.20 mL, 1.408 mmol, 4.5 eq.) are dissolved in dry THF (15 mL). Then, 15 (300.0 mg, 0.313 mmol, 1 eq.) is likewise dissolved in dry THF (20 mL) and added dropwise over 3 h at RT to the reaction solution. After further 60 min stirring at RT, the solvent is removed. The raw product is purified by column chromatography starting with cyclohexane : ethyl acetate 2 : 1 + 1% of glacial acetic acid, then the solvent is changed to CH_2Cl_2 followed by a change to CH_2Cl_2 : methanol 20 : 1 with a gradient to 10 : 1. The product fractions are collected and concentrated. The pure product is precipitated from ethanol, washed with ethanol, methanol, hexane and water. Yield: 170 mg (green-black solid, R_f (SiO$_2$; CH_2Cl_2 : methanol 10 : 1) = 0.41), 48%. λ_{max}(DCM)/nm = 835 (ε/M^{-1} cm^{-1} = 28 272), 611 (27 287), 403 (52 941). FT-IR (ATR): ν_{max}/cm^{-1} = 3476 (br), 2930 (w), 2210 (w), 1581 (m), 1500 (s), 1439 (w), 1323 (w), 1234 (m),

1171 (s), 1031 (m), 821 (m). ^{1}H-NMR (300 MHz, DMSO-d$_6$): δ/ppm = 1.13 (t, $^3J_{1H/1H}$ = 7.14 Hz, 6H, 2/6-CH$_2$CH_3), 2.49 (s, 6H, 1/7-CH_3), 2.67 (q, $^3J_{1H/1H}$ = 6.75 Hz, 4H, 2/6-CH_2CH$_3$), 3.75 (s, 12H, OMe), 6.76 (d, $^3J_{1H/1H}$ = 8.67 Hz, 4H, 3/5-H_{ar}), 6.92 (d, $^3J_{1H/1H}$ = 9.03 Hz, 8H, 3/5-H_{ar}), 7.05 (d, $^3J_{1H/1H}$ = 8.88 Hz, 8H, 3/5-H_{ar}), 7.20 (d, $^3J_{1H/1H}$ = 16.39 Hz, 2H, 3/5CH=CH), 7.38 (d, $^3J_{1H/1H}$ = 16.36 Hz, 2H, + d, 4H, $^3J_{1H/1H}$ = 8.22 Hz, 3/5CH=CH + 3/5-H_{ar}), 7.72 (d, $^3J_{1H/1H}$ = 8.22 Hz, 2H, 8-H_{ar}), 7.95 (d, $^3J_{1H/1H}$ = 8.34 Hz, 2H, 8-H_{ar}), 8.00 (s, 1H, Ph–CH=C(COOH)(CN)) ppm.

8-[(4-(1,3-Dioxolanyl)phenyl)ethynyl]-1,3,5,7-tetramethyl-2,6-diethyl-4,4-difluoro-4-bora-3a,4a-diaza-s-indacene (17). Under dry and oxygen-free conditions, 2-(4-iodophenyl)-1,3-dioxolane (4.54 g, 16.453 mmol, 3 eq.), Pd(PPh$_3$)$_4$ (0.38 g, 0.329 mmol, 0.06 eq.), CuI (4.2 mg, 0.219 mmol, 0.04 eq.) and NEt$_3$ (3.5 mL, 25.250 mmol, 4.7 eq.) are dissolved in dry THF (80 mL). Then, 11 (1.80 mg, 5.484 mmol, 1 eq.) is dissolved in dry THF (20 mL) and added dropwise over 3.5 h at RT to the reaction solution. After further 4 h stirring at RT, the solvent is removed. The residue is dissolved in CHCl$_3$ and washed with water (4 × 100 mL). The organic fraction is dried over Na$_2$SO$_4$ and filtered. After removal of the solvent, the raw product is purified by column chromatography with cyclohexane : ethyl acetate 6 : 1. Yield: 2.22 g (dark purple solid, R_f (SiO$_2$; cyclohexane : ethyl acetate 6 : 1) = 0.47), 85%. λ_{max}(DCM)/nm = 579 (ε/M^{-1} cm^{-1} = 30 887), 542 (15 910), 395 (16 874). FT-IR (ATR): ν_{max}/cm^{-1} = ^{1}H-NMR (300 MHz, DMF-d$_7$): δ/ppm = 1.08 (t, $^3J_{1H/1H}$ = 7.59 Hz, 6H, 2/6-CH$_2$CH_3), 2.44 (q, $^3J_{1H/1H}$ = 7.59 Hz, 4H, 2/6-CH_2CH$_3$), 2.51 (s, 6H, 3/5-CH_3), 2.54 (s, 6H, 1/7-CH_3), 4.00–4.20 (m, 4H, CH_2–CH_2), 7.54 (d, $^3J_{1H/1H}$ = 8.37 Hz, 2H, 8-H_{ar}), 7.59 (d, $^3J_{1H/1H}$ = 8.43 Hz, 2H, 8-H_{ar}).

Notes and references

1 A. Treibs and F.-H. Kreuzer, *Justus Liebigs Ann. Chem.*, 1968, **718**, 208.

2 D. Zhang, V. Martin, I. García-Moreno, A. Costela, M. E. Pérez-Ojeda and Y. Xiao, *Phys. Chem. Chem. Phys.*, 2011, **13**, 13026.

3 J. Karolin, L. B.-A. Johansson, L. Strandberg and T. Ny, *J. Am. Chem. Soc.*, 1994, **116**, 7801.

4 D. W. Domaille, L. Zeng and C. J. Chang, *J. Am. Chem. Soc.*, 2010, **132**, 1194.

5 K. Rurack, M. Kollmannsberger and J. Daub, *Angew. Chem., Int. Ed.*, 2001, **40**, 385.

6 L. Bonardi, H. Kanaan, F. Camerel, P. Jolinat, P. Retailleau and R. Ziessel, *Adv. Funct. Mater.*, 2008, **18**, 401.

7 R. K. Lammi, R. W. Wagner, A. Ambroise, J. R. Diers, D. F. Bocian, D. Holten and J. S. Lindsey, *J. Phys. Chem. B*, 2001, **105**, 5341.

8 G. Ulrich, R. Ziessel and A. Harriman, *Angew. Chem., Int. Ed.*, 2008, **47**, 1184.

9 A. Loudet and K. Burgess, *Chem. Rev.*, 2007, **107**, 4891.

10 R. Ziessel, G. Ulrich and A. Harriman, *New J. Chem.*, 2007, **31**, 496.

11 S. Kolemen, Y. Cakmak, S. Erten-Ela, Y. Altay, J. Brendel, M. Thelakkat and E. U. Akkaya, *Org. Lett.*, 2010, **12**, 3812.

12 S. Kolemen, O. A. Bozdemir, Y. Cakmak, G. Barin, S. Erten-Ela, M. Marszalek, J.-H. Yum, S. M. Zakeeruddin, M. K. Nazeeruddin, M. Grätzel and E. U. Akkaya, *Chem. Sci.*, 2011, **2**, 949.

13 D. Kumaresan, R. Thummel, T. Bura, G. Ulrich and R. Ziessel, *Chem.–Eur. J.*, 2009, **15**, 6335.

14 S. Erten-Ela, M. D. Yilmaz, B. Icli, Y. Dede, S. Icli and E. U. Akkaya, *Org. Lett.*, 2008, **10**, 3299.

15 T. Bura, N. Leclerc, S. Fall, P. Lévêque, T. Heiser, P. Retailleau, S. Rihn, A. Mirloup and R. Ziessel, *J. Am. Chem. Soc.*, 2012, **134**, 17404.

16 Y. Chen, L. Wan, D. Zhang, Y. Bian and J. Jiang, *Photochem. Photobiol. Sci.*, 2011, **10**, 1030.

17 V. Lin, S. DiMagno and M. Therien, *Science*, 1994, **264**, 1105.

18 Z. Liu, A. A. Yasseri, R. S. Loewe, A. B. Lysenko, V. L. Malinovskii, Q. Zhao, S. Surthi, Q. Li, V. Misra, J. S. Lindsey and D. F. Bocian, *J. Org. Chem.*, 2004, **69**, 5568.

19 G. S. Wilson and H. L. Anderson, *Synlett*, 1996, 1039.

20 C. O. Hann and A. Lapworth, *J. Chem. Soc. Trans.*, 1904, **85**, 46.

21 S. Bednarz and D. Bogdal, *Int. J. Chem. Kinet.*, 2009, **41**, 589.

22 M. Karas, I. Fournier and M. Bolte, *Acta Crystallogr., Sect. E: Struct. Rep. Online*, 2005, **61**, o383.

23 H. L. Kee, C. Kirmaier, L. Yu, P. Thamyongkit, W. J. Youngblood, M. E. Calder, L. Ramos, B. C. Noll, D. F. Bocian, W. R. Scheidt, R. R. Birge, J. S. Lindsey and D. Holten, *J. Phys. Chem. B*, 2005, **109**, 20433.

24 M. Thelakkat, R. Fink, P. Pösch, J. Ring and H.-W. Schmidt, *Polym. Prepr. (Am. Chem. Soc., Div. Polym. Chem.)*, 1997, **1**, 394.

25 K. Peter, H. Wietasch, B. Peng and M. Thelakkat, *Appl. Phys. A: Mater. Sci. Process.*, 2004, **79**, 65.

26 TURBOMOLE V6.3 2011, a development of University of Karlsruhe and Forschungszentrum Karlsruhe GmbH, 1989–2007, TURBOMOLE GmbH, since 2007; available from http://www.turbomole.com, 2007.

27 K. Willinger, K. Fischer, R. Kisselev and M. Thelakkat, *J. Mater. Chem.*, 2009, **19**, 5364.

28 N. M. Loim and E. S. Kelbyscheva, *Russ. Chem. Bull.*, 2004, **53**, 2080.

29 N. Tsuboya, M. Lamrani, R. Hamasaki, M. Ito, M. Mitsuishi, T. Miyashita and Y. Yamamoto, *J. Mater. Chem.*, 2002, **12**, 2701.

30 M. Sommer, S. Hüttner and M. Thelakkat, *Adv. Polym. Sci.*, 2010, **228**, 123.

31 L. Bonardi, G. Ulrich and R. Ziessel, *Org. Lett.*, 2008, **10**, 2183.